

## Local virial relation and velocity anisotropy for collisionless self-gravitating systems

Yasuhide SOTA<sup>1,2</sup>, Osamu IGUCHI<sup>1</sup>, Masahiro MORIKAWA<sup>1</sup> and Akika NAKAMICHI<sup>3</sup>

<sup>1</sup> *Department of Physics, Ochanomizu University, 2-1-1 Ohtuka, Bunkyo-ku, Tokyo, 112-8610, Japan*

<sup>2</sup> *Advanced Research Institute for Science and Engineering, Waseda University, Ohkubo, Shinjuku-ku, Tokyo, 169-8555, Japan*

<sup>3</sup> *Gunma Astronomical Observatory, 6860-86, Nakayama, Takayama, Agatsuma, Gunma, 377-0702, Japan*

The collisionless quasi-equilibrium state realized after the cold collapse of self-gravitating systems has two remarkable characters. One of them is the linear temperature-mass (TM) relation, which yields a characteristic non-Gaussian velocity distribution. Another is the local virial (LV) relation, the virial relation which holds even locally in collisionless systems through phase mixing such as cold-collapse. A family of polytropes are examined from a view point of these two characters. The LV relation imposes a strong constraint on these models: only polytropes with index  $n \sim 5$  with a flat boundary condition at the center are compatible with the numerical results, except for the outer region. Using the analytic solutions based on the static and spherical Jeans equation, we show that this incompatibility in the outer region implies the important effect of anisotropy of velocity dispersion. Furthermore, the velocity anisotropy is essential in explaining various numerical results under the condition of the local virial relation.

### §1. Introduction

The astronomical objects in our universe such as galaxies and clusters of galaxies are believed to be formed through the gravitational interactions among the mass elements composing these objects. These objects originated from tiny fluctuations around the almost homogeneous background achieve the virialized state through gravitational interactions with the time scale as short as the system's free-fall time. However, those with the scale larger than the size of a typical galaxy cannot achieve the thermal-equilibrium state, since the time-scale of the equilibrium becomes much longer than the age of our universe. These objects are called collisionless, since the collisional effect of the gravitational two-body encounters are much less effective than that of the gravitational mixing through the potential oscillation.

Collisionless self-gravitating systems (SGS) eventually settle down to a quasi-equilibrium state through the phase mixing and the violent relaxation processes under the potential oscillation.<sup>1)</sup> This quasi-equilibrium state is a prototype of the astronomical objects such as galaxies and clusters of galaxies. These objects often show universal profiles in various aspects.

The quasi-equilibrium states for SGSs have been well examined with N-body simulations both for the cold collapse simulations starting from the small virial ratio<sup>2)</sup> and for the cosmological simulations starting from the tiny fluctuations around the homogeneous expanding background.<sup>3)</sup> Here we pay our attention to the case with

the cold collapse and examine the common characters of the bound state through N-body simulations. Since the cold collapse is considered to be a typical case which causes the violent relaxation, it is meaningful to examine this typical case in order to grasp the universal character of violent relaxation as a first step.

When the system experiences violent gravitational processes such as cold collapse and cluster-pair collision, we obtained a universal velocity distribution profile expressed as the democratic (=equally weighted) superposition of Gaussian distributions of various temperatures (DT distribution hereafter) in which the local temperature  $T(r)$  is defined using the local velocity variance  $\langle v^2 \rangle$  as  $T(r) := m\langle v^2 \rangle(r)/3k_B$ , where  $m$  is the particle mass.<sup>4)</sup> Moreover, we have found that the locally defined temperature linearly falls down in the intermediate cluster region outside the central part, provided it is described against the cumulative mass  $M_r$ , *i.e.*,  $dT/dM_r = \text{const}$ . This fact is consistent with the appearance of DT distributions.

In addition to the linear TM relation, we have also obtained another peculiar fact that the LV relation between the locally defined potential energy and kinetic energy holds except for the weak fluctuations, that is, the local temperature  $T(r)$  is proportional to the local potential  $\Phi(r)$ , with constant proportionality  $6k_B T(r) = -m\Phi(r)$  for a wide class of cold collapse simulations.<sup>4),6)</sup>

In sec.2 we will show that the LV relation for SGS is supported by the results of a variety of cold collapse simulations and that among the spherical and isotropic models, polytropes with index  $n \sim 5$  with a flat boundary condition at the center are compatible with the numerical results except for the outer region of the bound state. In sec.3, we examine the anisotropic models under the condition of the LV relation. We will show that the analytical solutions exist under the LV condition with constant  $\beta$ . These analytical solutions can be utilized to form the simple model with the anisotropic velocity dispersion. Sec.4 is devoted to the summaries and conclusions of this paper.

## §2. LV relation and analysis with isotropic models

In the previous paper, we showed that linear TM relation is one of the remarkable characters of SGS bound states after a cold collapse.<sup>4)</sup> Here we pay our attention to another characteristic for SGS bound states, that is, the LV relation.

It is well known that the gravitationally bound system approaches a virialized state satisfying the condition

$$\overline{W} + 2\overline{K} = 0, \quad (2.1)$$

where  $\overline{W}$  and  $\overline{K}$  are, respectively, the averaged potential energy and kinetic energy of the whole bound system. This is a global relation that holds for the entire system, after the initial coherent motion fades out.

Here we define the locally averaged potential energy and kinetic energy inside the radius  $r$ , respectively as

$$\overline{W}_r \equiv \frac{1}{2} \int_0^r \Phi(r') \rho(r') 4\pi r'^2 dr', \quad (2.2)$$

$$\overline{K}_r \equiv \int_0^r \frac{\langle v^2 \rangle(r')}{2} \rho(r') 4\pi r'^2 dr', \quad (2.3)$$

where  $\star(r')$  means the local object  $\star$  evaluated at  $r'$ .

Then we extend the virial relation (2.1) locally as

$$\overline{W}_r + 2\overline{K}_r = 0, \quad (2.4)$$

and examine how precisely this relation is locally attained inside a bound state.

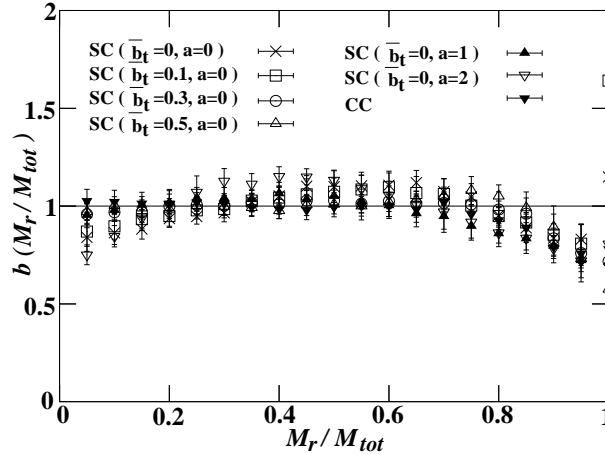


Fig. 1. The LV relation for some numerical simulations obtained by a typical cold collapse simulation; spherical collapse (SC) and cluster-pair collisions (CC). In the case of SC, 5000 particles are distributed with a power law density profile ( $\rho \propto r^{-a}$ ) within a sphere of radius  $R$  and the initial virial ratio ( $\bar{b}_t$ ) is set to be small. In the case of CC, each cluster has the equal number of particles (2500) and all particles are homogeneously distributed within a sphere of radius  $R$  and is set to be virialized initially. The initial separation of the pair is  $6R$  along the  $x$  axis. In all of the simulations, softening length  $\epsilon = 2^{-8}R$  is introduced to reduce the numerical error caused by close encounters. The local virial ratio  $b$  is plotted as a function of  $M_r/M_{tot}$ , where  $M_{tot}$  is the total mass of the system. The virial ratios at  $M_r$  are time averaged from  $t = 5t_{ff}$  and  $t = 100t_{ff}$ .

More precisely, the above relation Eq.(2.4) is equivalent to the purely local relation

$$2\langle v^2 \rangle(r) = -\Phi(r), \quad (2.5)$$

at each position  $r$ . Hence, we define the LV ratio

$$b(r) \equiv -2\langle v^2 \rangle(r)/\Phi(r), \quad (2.6)$$

and examine the value of  $b(r)$  for each shell. For a wide class of collapses including cluster-pair collision,<sup>4)</sup> the value  $b(r)$  takes almost unity: it deviates from unity less than 10 percent upward in the intermediate region and a little more downward in the inner and outer region for all of the simulations (Fig.1). Hence a wide class of cold collapse simulations yield the relation (2.5) quite well. This LV relation should be another characteristic of SGS, in addition to the linear TM relation.

From a viewpoint of these two characteristics, we compared our results with polytropes. The polytrope with  $n = 5$  is special among those models, since it exactly satisfies the LV relation (Fig.2). Moreover, it admits the analytical solution called Plummer's model under the condition that the potential is flat at the center of the system.<sup>5)</sup> We got the result that Plummer's model satisfies the linear TM relation quite well in the intermediate region  $0.2M_{tot} < M_r < 0.8M_{tot}$ .<sup>6)</sup> On the other hand, both its TM relation and density profile in the outer region differ from the ones derived in cold collapse simulations: the temperature falls off more steeply and the density behaves as  $r^{-5}$  in the outer region.

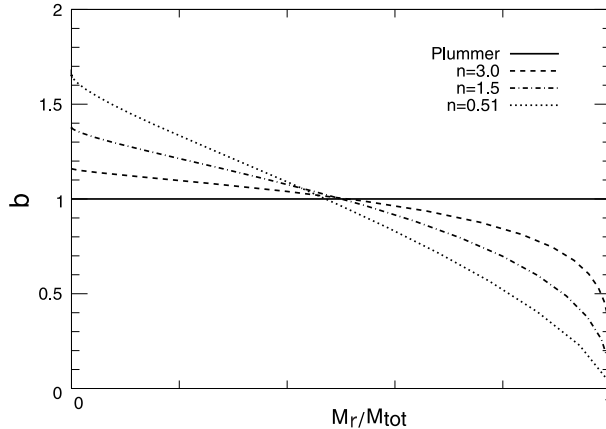


Fig. 2. LV relation for polytropes. The solid curve refers to the LV ratio  $b(M_r/M_{tot})$  as a function of cumulative mass  $M_r/M_{tot}$  for Plummer's model. The other curves refer to  $b(M_r/M_{tot})$  for polytropes with  $n = 3.0$  (dashed),  $n = 1.5$  (dot-dashed), and  $n = 0.51$  (dotted).

### §3. Models with anisotropic velocity dispersion

In the previous section, we commented that Plummer's model expresses the bound state quite well after a cold collapse among the spherical systems with isotropic velocity dispersion. However, it fails in explaining the outer region of the bound state, where the velocity dispersion is anisotropic (Fig.3). Here we pay our attention to this anisotropy and examine the general static Jeans equation admitting this anisotropy.

In the collisionless system, the particle distribution can be described by the Vlasov equation. Integrating the spherical and static Vlasov equation in velocity space after multiplying  $v_r$  results in the spherical and static Jeans equation,

$$\frac{d(\rho \langle v_r^2 \rangle)}{dr} = \rho \frac{d\phi}{dr} - \frac{2 \langle v_r^2 \rangle \beta \rho}{r}, \quad (3.1)$$

where  $\beta \equiv 1 - (\langle v_\theta^2 \rangle + \langle v_\phi^2 \rangle) / (2 \langle v_r^2 \rangle)$  is the anisotropy parameter and  $\phi$  is the relative potential defined as  $\phi \equiv \Phi_* - \Phi$ , where  $\Phi_*$  is the maximum energy of the particles in the system.<sup>5)</sup>

Assuming that the density is non-zero everywhere but the total mass is finite, we can get the condition that  $\Phi_* = 0$ . In this case, from the condition that  $\langle v^2 \rangle =$

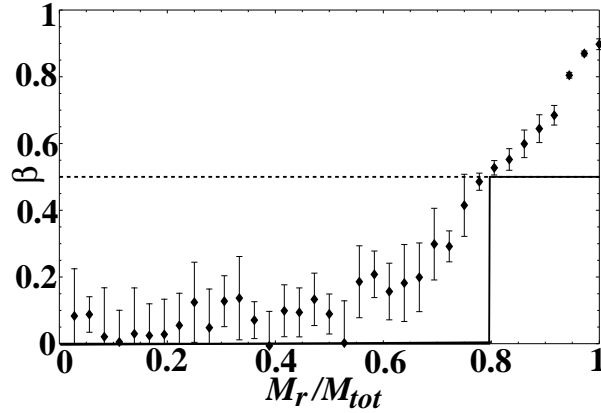


Fig. 3. The distribution of the anisotropy parameter  $\beta(r)$ . A plot with error-bar is the result of the numerical simulation SC with  $(\bar{b}_t, a) = (0, 0)$  but with  $N = 10000$  in Fig.1. A solid thick line represents the combined solution (A-1) with  $c = 0.2$  and a dot line represents the analytical solution with  $\beta = 0.5$ .

$(3 - 2\beta) \langle v_r^2 \rangle$ , the LV relation (2.5) takes the form of

$$\langle v_r^2 \rangle = \frac{\tau}{2} \phi, \quad (3.2)$$

where  $\tau \equiv 1/(3 - 2\beta)$ . From Eqs. (3.1) and (3.2), we derive the relation

$$\frac{d(\tau\rho\phi)}{dr} = 2\rho \frac{d\phi}{dr} - \frac{(3\tau - 1)\rho\phi}{r}. \quad (3.3)$$

The relative potential also follows the Poisson's equation

$$\frac{1}{r^2} \frac{d}{dr} \left( r^2 \frac{d\phi}{dr} \right) = -4\pi^2 G\rho. \quad (3.4)$$

Eqs.(3.3) and (3.4) are basic equations for  $\phi$  and  $\rho$  when the anisotropy parameter  $\beta$  is given.

The equation (3.3) is integrable under the condition that  $\beta$  is constant, which leads to the relation

$$\rho = A\phi^{5-4\beta} r^{-2\beta}, \quad (3.5)$$

where  $A$  is an integral constant. Substituting Eq.(3.5) into Eq.(3.4), we can get the nonlinear equation for  $\phi$ , which admits the analytical solution

$$\phi(r) = \frac{GM_{tot}}{(r^s + r_0^s)^{1/s}}, \quad (3.6)$$

where  $s \equiv 2(1 - \beta)$  and  $r_0 \equiv \left(\frac{4\pi GA}{s+1}\right)^{1/s} M_{tot}^2$  under the boundary condition at infinity;

$$\begin{aligned} \phi(\infty) &= \rho(\infty) = 0 \\ \frac{d\phi}{dr} \Big|_{r \rightarrow \infty} &= -\frac{GM_{tot}}{r^2} \end{aligned} \quad (3.7)$$

.<sup>7)</sup> We will analyze more general solutions for eq. (3·1) and (3·4) under the constant LV ratio  $b$  in another paper.<sup>8)</sup>

Especially when  $\beta = 0$ , the solution (3·6) is nothing but Plummer's model. The Plummer's model explains several characters of the bound state after a cold collapse or cluster-pair collisions quite well except for the outer region. Here we compare this solution with the solution connecting inner Plummer's solution with the outer analytical solution with constant  $\beta$  (See Appendix A). Of course, the actual function form of  $\beta(r)$  is too complicated to be expressed by the connection of several constant  $\beta$  analytical solutions. However, we can roughly see that considering the anisotropy reduce the incompatibility of the solution to the bound state after a cold collapse (Fig.4 and Fig.5).

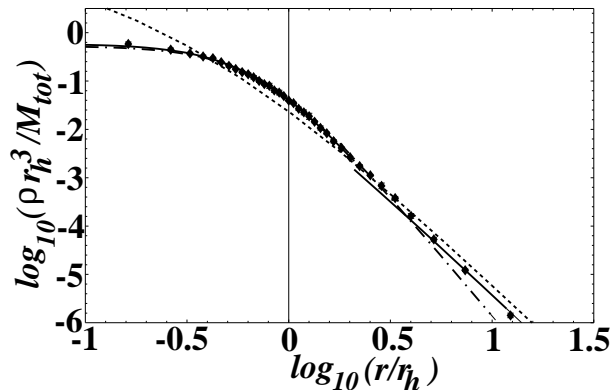


Fig. 4. A log-log plot for a density profile with the unit of  $r_h = M_{tot} = G = 1$ , where  $r_h$  is the half-mass radius of the bound system. A plot with error-bar is the result of the numerical simulation SC with  $(\bar{b}_t, a) = (0, 0)$  but with  $N = 10000$  in Fig.1. A solid line represents the combined solution (A·1) with  $c = 0.2$ . A dot and dot-dashed line represent the analytical solution with  $\beta = 0.5$  and the Plummer's model, respectively. The coincidence between numerical data and the combined solution is remarkable.

#### §4. Conclusions

The bound states after a cold collapse or several other initial conditions with small initial virial ratio are characterized by the linear temperature-mass (TM) relation and the local virial (LV) conditions. Among the spherical and static models as the solution of Vlasov equation with isotropic velocity dispersion, the polytrope with  $n = 5$  is very special, since it satisfies the LV relation exactly. Plummer's solution, which is the analytical solution of polytrope with  $n = 5$  satisfying the flat boundary condition at the center explains several characters of the bound state quite well except for the outer region. Here we showed that this incompatibility can be reduced by adding the anisotropic effect under the condition of the LV relation. This leads to the result that the bound state after a cold collapse characterized by the density profile with the asymptotic form  $\propto r^{-4}$  and linear TM relation can be explained quite well by the anisotropic model satisfying the LV relations.

Here we have restricted our analysis to cold collapse models with small initial

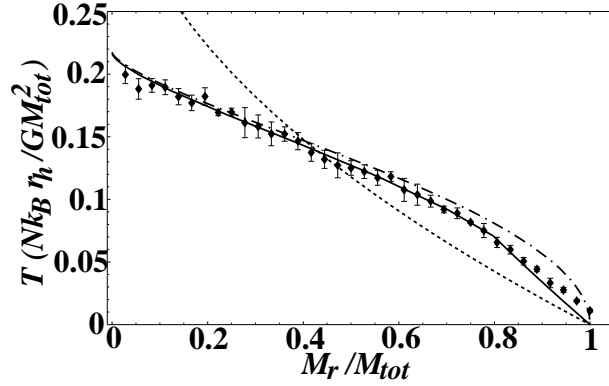


Fig. 5. A Temperature-Mass relation with the unit of  $r_h = M_{tot} = G = 1$ , where  $r_h$  is the half-mass radius of the bound system. A plot with error-bar is the result of the numerical simulation SC with  $(\bar{b}_t, a) = (0, 0)$  but with  $N = 10000$  in Fig.1. A solid line represents the combined solution (A.1) with  $c = 0.2$ . A dot and dot-dashed line represent the analytical solution with  $\beta = 0.5$  and the Plummer's model, respectively. The coincidence between numerical data and the combined solution is remarkable.

virial conditions. However, it seems important how widely our results are applicable in more general mixing processes including merging process in cosmological simulations. It is well known that the bound states observed in cosmological simulations are quite different from those in cold collapse. For example, the density has the central cusp  $\propto r^{-1}$  and takes the outer asymptotic form  $\propto r^{-3}$  in cosmological simulations.<sup>3)</sup> Moreover, the phase space density defined as  $\rho/\sigma^3$  has a single power-law property in radius.<sup>9)</sup> Hence it seems important to see if the LV relation is admitted even in the case with such different characters. These points are now under investigation.<sup>8)</sup>

## Appendix

Here we connect the two analytical solution at  $r = r_c$ , i.e., Plummer's model ( $\beta = 0$ ) for  $r \leq r_c$  and  $\beta = 0.5$  analytical solution for  $r \geq r_c$ . Defining  $\phi_c \equiv \phi(r_c)$  and describing the physical quantities with the unit of  $r_c = \phi_c = G = 1$ , the connected solution is described with one-parameter  $c$  as

$$\phi(r) = \begin{cases} \sqrt{\frac{1+3c^2}{r^2+3c^2}} & (r \leq 1) \\ \frac{1+3c^2}{r+3c^2} & (r > 1) \end{cases}, \quad (\text{A.1})$$

from the continuity condition of  $\phi(r)$  and  $d\phi(r)/dr$  at  $r=1$ .

Inner Mass  $M(r) = r^2 d\phi/dr$  becomes

$$M(r) = \begin{cases} \frac{\sqrt{1+3c^2}r^3}{\sqrt{(r^2+3c^2)^3}} & (r \leq 1) \\ \frac{(1+3c^2)r^2}{(r+3c^2)^2} & (r > 1) \end{cases}. \quad (\text{A.2})$$

Hence the total mass  $M_{tot}$  is described as

$$M_{tot} = \lim_{r \rightarrow \infty} M(r) = 1 + 3c^2.$$

The mass ratio between the total mass of inner Plummer region,  $M_{plum}$  and  $M_{tot}$  becomes

$$\frac{M_{plum}}{M_{tot}} = \frac{1}{(1 + 3c^2)^2}.$$

Hence the parameter  $c$  determines the mass ratio of the connected two regions.

#### References

- 1) Lynden-Bell D., MNRAS **136** (1967), 101.
- 2) Van Albada T.S., MNRAS **201** (1982), 939.
- 3) Navarro J. F., Frenck C. S. and White S. D. M., Astrophys. J. **462** (1996), 563.
- 4) Iguchi O., Sota Y., Tatakawa T., Nakamichi A. and Morikawa M., Phys. Rev. **E71** (2005), 016102.
- 5) Binney J. J. and Tremaine S., Galactic Dynamics (Princeton University Press, Princeton, 1987).
- 6) Sota Y., Iguchi O., Morikawa M. and Nakamichi A astro-ph/0403411.
- 7) Evans N. W. and An J., MNRAS **360** (2005) 492.
- 8) Iguchi O., Sota Y., Morikawa M. and Nakamichi A (in preparation).
- 9) Taylor J. E. and Navarro J. F., Astrophys. J. **563** (2001), 483.